HHS Public Access

Author manuscript

Chem Res Toxicol. Author manuscript; available in PMC 2025 May 16.

Published in final edited form as:

Chem Res Toxicol. 2023 May 15; 36(5): 747–756. doi:10.1021/acs.chemrestox.2c00407.

Chemistry of Isoeugenol and Its Oxidation Products: Mechanism and Kinetics of Isoeugenol as a Skin Sensitizer

Jongmin Ahn,
National Center for Natural Products Research, Research Institute of Pharmaceutical Science, School of Pharmacy, The University of Mississippi, University, Mississippi 38677, United States; Natural Product Research Center & Natural Product Central Bank, Korea Research Institute of Bioscience and Biotechnology (KRIBB), Cheongju 28116, Republic of Korea

Cristina Avonto,
National Center for Natural Products Research, Research Institute of Pharmaceutical Science, School of Pharmacy, The University of Mississippi, University, Mississippi 38677, United States; Firmenich Inc., Plainsboro Township, New Jersey 08536, United States

Pankaj Pandey,
National Center for Natural Products Research, Research Institute of Pharmaceutical Science, School of Pharmacy, The University of Mississippi, University, Mississippi 38677, United States

Shabana I. Khan,
National Center for Natural Products Research, Research Institute of Pharmaceutical Science, School of Pharmacy and Division of Pharmacognosy, Department of BioMolecular Sciences, School of Pharmacy, The University of Mississippi, University, Mississippi 38677, United States

Ikhlas A. Khan,
National Center for Natural Products Research, Research Institute of Pharmaceutical Science, School of Pharmacy and Division of Pharmacognosy, Department of BioMolecular Sciences, School of Pharmacy, The University of Mississippi, University, Mississippi 38677, United States

David W. Roberts,
School of Pharmacy and Biomolecular Sciences, Liverpool John Moores University, Liverpool L3 3AF England, U.K.

Amar G. Chittiboyina
National Center for Natural Products Research, Research Institute of Pharmaceutical Science, School of Pharmacy, The University of Mississippi, University, Mississippi 38677, United States

Abstract

Corresponding Author Amar G. Chittiboyina – *National Center for Natural Products Research, Research Institute of Pharmaceutical Science, School of Pharmacy, The University of Mississippi, University, Mississippi 38677, United States*; amar@olemiss.edu; Fax: 1-662-915-7989.

ASSOCIATED CONTENT

Supporting Information

The Supporting Information is available free of charge at https://pubs.acs.org/doi/10.1021/acs.chemrestox.2c00407.

Kinetic ^{1}H NMR data of the adducts, DP4+, CP3, spectral data, and relative energies for compounds **3a**, **3b**, **4a**, and **4b** (PDF)

The authors declare no competing financial interest.

Structurally similar phytochemical compounds may elicit markedly different skin sensitization responses. Eugenol and isoeugenol are natural phenylpropanoids found in various essential oils are frequently used as fragrance ingredients in consumer products due to their pleasing aromatic properties. Both compounds are also skin sensitizers with isoeugenol being a stronger sensitizer than eugenol. The most commonly accepted mechanisms for haptenation by eugenol involve formation of a quinone methide or an *ortho*-quinone intermediate. The mechanism for the increased skin response to isoeugenol remains elusive, although quinone methide intermediates have been proposed. The recent identification of diastereomeric 7,4′-oxyneolignans as electrophilic, thiol-depleting isoeugenol derivatives has revived interest in the possible role of elusive reactive intermediates associated with the isoeugenol's haptenation process. In the present work, integrated non-animal skin sensitization methods were performed to determine the ability of *syn*-7,4′-oxyneolignan to promote haptenation and activation of further molecular pathways in keratinocytes and dendritic cells, confirming it as a candidate skin sensitizer. Kinetic NMR spectroscopic studies using dansyl cysteamine (DCYA) confirmed the first ordered nature of the nucleophilic addition for the *syn*-7,4′-oxyneolignan. Computational studies reaffirmed the "*syn*" stereochemistry of the isolated 7,4′-oxyneolignans along with that of their corresponding DCYA adducts and provided evidence for the preferential stereoselectivity. A plausible rationale for isoeugenol's strong skin sensitization is proposed based on the formation of a hydroxy quinone methide as a reactive intermediate rather than the previously assumed quinone methide.

Graphical Abstract

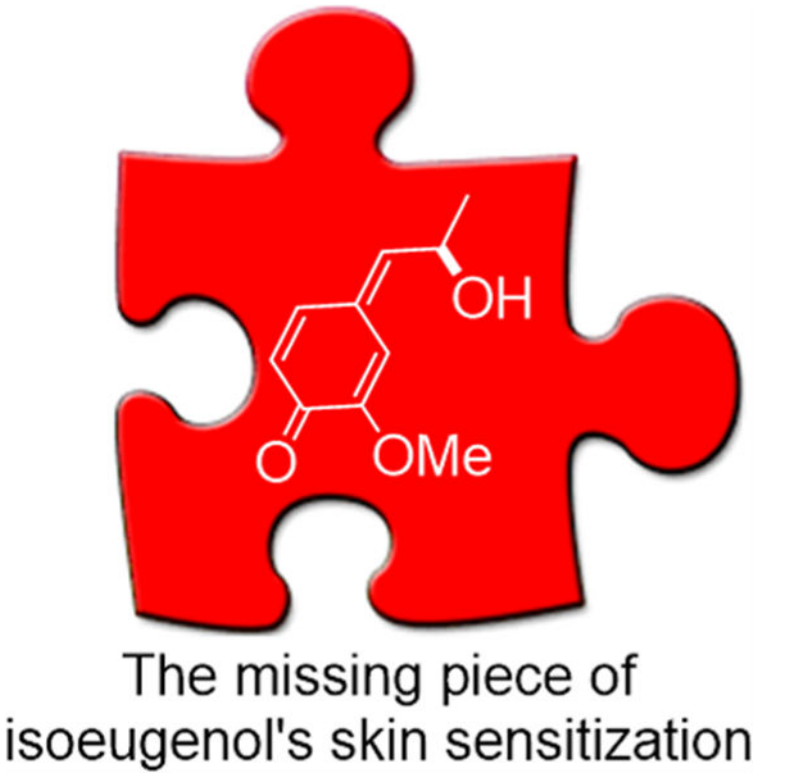

1. INTRODUCTION

Naturally occurring isoeugenol and its structural analogue eugenol are volatile constituents of various essential oils, especially clove (*Eugenia caryophyllata*). The cosmetic and fragrance industries use isoeugenol and eugenol extensively as a woody-spicy note in fine fragrance bouquets, household products, and as flavoring agents in oral formulations such as over-the-counter medicines.[1,2] For isoeugenol alone, more than 1500 beauty and personal care products are listed in the Mintel Global New Products Database; about 50% of those products were registered within the last 5 years.

Although renowned in the fragrance industry due to its desirable organoleptic properties, isoeugenol is also a dermatologic sensitizer (or contact allergen). Allergic reactions to isoeugenol are so widespread that the compound was included in the fragrance mix I used in routine allergen patch tests. The International Fragrance Association (IFRA) has recommended isoeugenol concentrations below 200 ppm in final products.[3] Despite such restrictions, White et al.[4] reported an increased incidence of isoeugenol-related skin allergies and attributed this phenomenon to its substitution with ester derivatives such as isoeugenyl acetate and isoeugenyl phenylacetate, each of which can generate isoeugenol *via* hydrolysis *in situ*.

The isoeugenol molecule lacks typical structural prerequisites necessary for covalent binding to skin proteins *via* a mechanism referred to as the Molecular Initiating Event (MIE) of the Adverse Outcome Pathway (AOP) for skin sensitization.[5] It has been hypothesized that either biotic activation by skin enzymes[6] or abiotic activation through its rapid oxidation may be involved in inducing and eliciting skin sensitization.[7] Isoeugenol, a colorless oil when purified, becomes yellow and viscous upon extended storage. Isoeugenol is regarded as a stronger sensitizer than eugenol,[8] and clinical evidence seems to corroborate laboratory findings.[9] The differential skin sensitization potency of the two compounds has attracted many dermato-toxicologists, yet the exact mechanism is largely unknown. Isoeugenol, eugenol, and their structural analogues have been the subject of several mechanistic studies,[10–12] and *in vivo* experiments highlighted the significant differences in sensitization properties, both in animal (guinea pig tests and LLNA) and in human predictive studies. It has been proposed that skin sensitization of eugenol may involve metabolic demethylation, followed by oxidation to the corresponding *ortho*-quinone. This is in contrast to the proposed isoeugenol pathway that involves direct oxidation to the corresponding *para*-quinone methide (QM)[6] as depicted in Figure 1, despite the potential for both isoeugenol and eugenol to yield the same QM as a reactive intermediate.

An electrophilic QM intermediate could react as a Michael acceptor and thus mechanistically justify the observed chemical reactivity of **1** with thiol- and amino-based peptides.[13] Haptenation *via* QM could explain why isoeugenol is a stronger sensitizer than eugenol if the reasonable assumption is made that the demethylation of eugenol or the direct oxidation to a QM is less favorable compared to the oxidation of isoeugenol. However, it is not obvious why eugenol oxidation to a QM should be less favored. A difference in the chemical pathways is implied by clinical evidence of the lack of cross-reactivity. Indeed,

patch tests on allergic individuals have often reported sensitization reactions to one, but not both, of these fragrances.[6]

Despite the evidence from *in vivo* studies, the lack of experimental characterization of QM adducts complicates the validity of the QM hypothesis. We recently reported[14] an important piece of evidence by identifying a reactive, electrophilic *syn*-7,4′-oxyneolignan (**3a**), which is an oxidized dimeric derivative of isoeugenol found in a commercial isoeugenol sample (trace) and separately obtained *via* forced degradation (photo-induced oxidative conditions). The general structure of this oxidation compound of isoeugenol was previously reported as an olfactory receptor antagonist.[15] Stability–reactivity studies of the newly isolated compound showed that isoeugenol is moderately unstable under forced degradation,[15] resulting in greater, time-dependent, thiol reactivity.[16] The chemical reactivity of **3a** and isoeugenol, together with the absence of classic mechanistic domains, warrants deeper investigation into the two compounds' reactivity that could originate from a common reactive intermediate, *viz.*, QM, or through the involvement of other reactive, transient intermediates.

Studying unstable reactive intermediates with a short half-life is inherently challenging. However, NMR kinetic methods have the advantage of providing structural insights on the reaction mechanism by monitoring the reaction progress in real time without the need to perform isolation procedures. Previously, the utility of an NMR-based *in chemico* method using dansyl cysteamine (NMR-DCYA) was effectively demonstrated to characterize and classify the reactivity of potential skin sensitizers, either as a single compound[17,18] or as complex mixtures.[19,20] This method provides direct structural information about the hapten adducts and significantly differs from the other *in chemico* methods currently used and accepted as test guidelines for non-animal sensitization, where chromatographic methods indirectly infer the sensitization potentials based on depletion of thiol- or amino-based nucleophiles. Particularly, NMR-DCYA is advantageous because other methods endorsed by the regulatory agencies cannot provide the same degree of direct evidence to explain the plausible mechanism associated with potential skin sensitizers.

In the present work, nucleophilic addition of DCYA to 7,4′-oxyneolignans was undertaken to answer unresolved mechanistic dilemma associated with isoeugenol. Kinetic NMR experiments, together with testing of oxyneolignans using non-animal methods, *viz.*, direct peptide reactivity assay (DPRA), KeratinoSens, and human cell line activation assay (h-CLAT), were conducted to comprehend the increased skin sensitization with isoeugenol and to elucidate the potential role of reactive intermediates in clinically established dermatological effects.

2. MATERIALS AND METHODS

2.1. Reagents and Instrumentation.

Isoeugenol **1** (CAS. 97-54-1), 2,5-dimethyl furan (DMF), and 1,5-diazabicyclo[4.3.0]non-5-one (DBN) were purchased from Sigma-Aldrich (St. Louis, MO, USA). Deuterated chloroform ($CDCl_3$) was purchased from Cambridge Isotope Laboratories (Tewksbury, MA, USA). The fluorescent compound DCYA and its disulfide $(DCYA)_2$ were synthesized as

described previously.[18] The kinetic NMR studies were performed using an Agilent 500 MHz spectrometer (Agilent Technologies, Santa Clara, CA, USA).

Polymer-supported maleimide was purchased from SiliCycle (Quebec City, Quebec, Canada). Standardized pH 10 buffer and HPLC-grade acetonitrile (ACN) were purchased from Fisher Scientific (Suwanee, GA, USA). Flash chromatography purifications were achieved with an Isolera Four system (Biotage, Uppsala, Sweden) equipped with either Biotage or SiliCycle silica gel flash cartridges. Controls used for the HTS assay (cinnamaldehyde, coumarin, and massoia lactone) were purchased from Sigma-Aldrich, St. Louis, MO, USA. Cysteine peptide (94.9%, cat. N. RSC998) and lysine peptide (91.1%, cat. N. RSC999) were purchased from RS Synthesis (Louisville, KY, USA). Sodium phosphate buffer (Na_2HPO_4/NaH_2PO_4, 100 mM pH 7.4) was used for Cys-DPRA stock solutions and reactions; ammonium acetate buffer (CH_3COONH_4/NH_4OH, 100 mM pH 10.2) was used for the Lys-DPRA peptide. HPLC grade ACN was used for both HTS-DCYA and DPRA experiments.

Analytical HPLC-DAD-MS data were acquired using an Agilent Infinity 1290 system equipped with a quaternary pump, an autosampler, a thermoregulated multi-column compartment, a photodiode array detector, and a single-quadrupole mass spectrometer. Data were acquired using Agilent Open Lab ChemStation data acquisition software (Agilent Technologies). A ZORBAX Eclipse Plus C18, 3 × 150 mm, 3.5 μm column was used with a binary solvent system (water and methanol, both containing 0.1% formic acid). The initial percentage of MeOH was 60%, increased to 80% in 4 min, then to 90% in 5 min, and to 95% B in 3 min, holding for 4 min. The flow rate was set at 0.250 mL/min, and UV was monitored at 254 and 330 nm. Positive and negative ESI spectra were acquired from 100 to 1000 amu.

2.2. Isolation and Characterization of 7,4′-Oxyneolignans (3a and 3b) from Aged Isoeugenol.

Seventeen grams of isoeugenol was exposed to light for five weeks under constant airflow with six h dark/light cycles (forced degradation). Photo-induced oxidation with air for 100 days resulted in 40% degradation. Forced degradation for 35 days provided a sufficient amount of oxidized isoeugenol for this study. The degradation byproducts were isolated on silica gel using SNAP HP-Sil flash cartridges (Biotage) eluted with 100% chloroform. The major *syn*-7,4′-oxyneolignan **3a** (1.8 g, 10.5%) and the minor diastereomer **3b** (253.3 mg, 1.5%) were isolated, and their structures were confirmed by NMR (Table S1 and Figure S1), mass spectrometry, and comparison with previously reported data.[14] The relative stereochemistry was further confirmed by computational methods as outlined in Section 2.3.

2.3. Computational Studies.

^1H and ^{13}C NMR chemical shift calculations were performed to assign the relative configuration for C-7 and C-8 on the compounds **3a**/**3b** (Tables S2–S7) and C-7″ and C-8″ on **3a**-DCYA adduct **4a** (Tables S8–S10) using the CP3 (http://www-jmg.ch.cam.ac.uk/tools/nmr/CP3.html) and DP4+ (https://sarotti-nmr.weebly.com) probability analysis.[21,22] The ligand preparation (3D energy-minimized structure), conformational search, and

geometry optimizations of the above compounds were performed using the procedure described earlier.[23,24] In brief, the 2D structures of compounds (7*R*,8*R*)-7,4′-oxyneolignans (**3**), (7*S*,8*R*)-**3**, (7″*R*,8″*R*)-DCYA-adducts (**4**), and (7″*S*,8″*R*)-**4** were drawn to include*syn*-**3**, *anti*-**3**, *syn*-**4**, and *anti*-**4**, respectively, in the 2D sketcher module of Maestro 12.6.144 (Schrödinger LLC, New York, NY, USA). The structures were prepared at physiological pH 7.4 with the LigPrep module implemented in the Schrödinger software (Schrödinger LLC, New York, NY, USA) using the OPLS3e force field.[25] The conformational search of the above compounds was performed in $CHCl_3$ with the MacroModel program implemented in Schrödinger using the Mixed torsional/Low mode sampling method. An energy cutoff of 10 kcal/mol was used to cover all the possible lowest energy conformers. The gauge-independent atomic orbital (GIAO) NMR method[26] at the DFT mPW1PW91/6−311+G(d,p) level of theory was used for DP4+/CP3 calculations, including the chemical shift calculations (^{1}H and ^{13}C) using Boltzmann weighting for all low-energy conformations (Table S11). $CHCl_3$ (the solvent used experimentally) was used as the solvent with the polarizable continuum solvent model (PCM).[27] The geometry optimization and NMR calculations were performed using Gaussian 16 Rev. B. 01 (Gaussian, Inc., CT, USA). The computed chemical shifts of compounds *syn*-**3**, *anti*-**3**, *syn*-**4**, and *anti*-**4** were compared with the corresponding experimental ^{1}H and ^{13}C NMR chemical shifts, utilizing corrected mean absolute error (CMAE) and CP3/DP4+ probability analyses (Tables S2, S8 and S7). The scaled chemical shifts were calculated by applying empirical scaling using the slope and intercept of the regression line obtained by plotting the chemical shift values of ^{1}H and ^{13}C (calculated vs experimental).

2.4. Integrated Skin Sensitization Testing Using Non-animal Methods.

2.4.1. Direct Peptide Reactivity Assay. The MIE in the AOP is considered to be the covalent bonding of electrophilic chemicals to nucleophilic centers in skin proteins. Characterization of the MIE was evaluated using the DPRA method as described by the Organisation for Economic Co-operation and Development (OECD) Guideline 442C.[28] Peptide depletion was estimated based on an average of three independent experiments. Cinnamaldehyde was used as the positive control, and ACN was used as the solvent control. Cys-peptide and Lys-peptide were prepared with 0.1 M potassium phosphate buffer at pH 7.4 and 0.1 M ammonium acetate buffer at pH 10.2, respectively, before use. Analyses were performed using an Agilent Infinity 1290 HPLC-DAD system. Data were acquired using the Agilent Open Lab ChemStation data acquisition software (Agilent Technologies). A ZORBAX SB-C-18 (2.1 × 150 mm, 3.5 μm column) was used with 0.1% [v/v] trifluoroacetic acid (TFA) in water (solvent A) and 0.085% [v/v] TFA in ACN (solvent B) at 30 °C. The flow rate was adjusted to 0.35 mL/min. Gradient elution was carried out as follows: linear gradient from 10 to 25% of solvent B for 10 min, followed by a rapid increase to 90% B in 1 min and then from 90 to 100% B in 1 min. Absorbance at 220 nm was used to determine the peptide depletion.

2.4.2. KeratinoSens (ARE-Nrf2 Luciferase Assay). The second key event in the AOP occurs in the keratinocyte and includes inflammatory responses and expression of specificgenes. The KeratinoSens is an *in vitro* assay that uses the luciferase reporter gene for the detection of activation of the Keap1-Nrf2 signaling pathway, which was discovered

to be activated during skin sensitization events.[29] The KeratinoSens assay was performed as described by OECD Guideline 442D.[30] The cell line was obtained from Givaudan (Vernier, Switzerland) and maintained in our laboratory per the supplier's recommendations. In brief, cells were cultured in DMEM supplemented with GLUTAMAX, 10% fetal bovine serum, and G418 500 μg/mL at 37 °C with 5% CO_2, and 95% humidity. Upon 80–90% confluency, the cells were suspended in a 10% FBS antibiotic-free medium and seeded in multiple 96-well tissue culture-treated microplates for the luciferase assay and one clear 96-well plate for toxicity assessments. Cinnamaldehyde was used as a positive control, while DMSO (1%) was used as a vehicle control in the assay. The cell viability was calculated as a percent of control, and the concentration responsible for 50% cell death (TC_{50}) was calculated from the dose–response curves of cell viability *versus* concentrations of tested samples. The $EC_{1.5}$ value (the concentration responsible for the 1.5-fold increase in luciferase activity) was calculated based on the equation shown below

$$EC_{1.5} = (C_b - C_a) \times \frac{1.5 - I_a}{I_b - I_a} + C_a$$

where C_a is the concentration above 1.5-fold induction, C_b is the concentration below 1.5-fold induction, I_a is the fold induction above 1.5-fold induction, and I_b is the fold induction below 1.5-fold induction.

2.4.3. Human Cell Line Activation Assay (h-CLAT). The third key event in the AOP is the activation of dendritic cells. The h-CLAT assay was performed in THP-1 cells (obtained from ATCC) per the OECD Guideline 442E.[31] In brief, the cells were cultured in RPMI 1640 media supplemented with 10% FBS, 0.05 mM 2-mercaptoethanol, and 1% antibiotic-antimycotic (Fisher Scientific). Test compounds were dissolved in DMSO (250 mg/mL). DNCB (1-chloro-2,4-dinitrobenzene, Sigma-Aldrich) was included as a positive control in each experiment. The concentration to maintain at least 75% cell viability (CV75) was established for each compound, and the relative fluorescence intensities (RFIs) of CD86 and CD54 were calculated. If the RFI of CD86 or CD54 was greater than 150 or 200%, respectively, at any dose in at least two experiments, the test chemical was judged as a sensitizer.

2.5. NMR-DCYA Method.

Kinetic experiments were performed by the sequential acquisition of ^{1}H NMR spectra at predetermined time intervals.[18] The general acquisition parameters were set as follows: the delay time was 20 s, pulse width 30°, temperature fixed at 25 °C, four scans, and 0.20 Hz FID resolution. The chemical shifts are reported in ppm relative to the residual ^{1}H solvent signal ($CDCl_3$ δ 7.26 ppm). Dimethylfuran 33 mM was used as an internal standard (IS). A solution of DCYA in $CDCl_3$ (125 μL) was mixed with an equal volume of the test compound in $CDCl_3$ containing IS. The control reaction was monitored every 5 min for 30 min. Then, the experimental reaction was initiated by adding 12.5 μL of DBN (200 mM in $CDCl_3$, 0.2 equiv. final concentration), and additional proton spectra were recorded every 5 min for at least 50 min (Figures S2 and S3).

The acquired spectra were processed and analyzed using MNOVA v.12.0.4 and MS Office Excel 365. The data were pre-processed by baseline and noise correction. The area of different proton signals was selected for reactants and products, and the values were normalized against the aromatic signal of the IS (δ 5.82, s, 2H) and averaged. The reaction times were adjusted for the acquisition lag time, defined as the time interval between the addition of DBN to the reaction tube and the acquisition of the first reaction ^{1}H spectrum. The reaction results were then reported as depletion of the electrophile signal (doEs)[18]

$$\text{doEs} = 100\% \frac{\int C_x \times \int \text{IS}_0}{\int \text{IS}_x \times \int C_0}$$

where C_x = area of the signal of interest of the compound(s) at a defined time x, C_0 = area of the signal of interest of the compound at time 0, IS_0 = area of the internal standard peak at 5.82 ppm at time 0, and IS_x = area of the internal standard peak at time x. The doEs were calculated based on the average of three independent repetitions.

3. RESULTS

3.1. Confirmation of Relative Configuration of 3a, 3b, and 4a.

In an attempt to understand the differential skin sensitization potentials of isoeugenol and its elusive reactive intermediates, we previously performed a stability–reactivity study.[16] Interestingly, eugenol was identified as less susceptible to oxidative degradation, with only a moderate increase in reactivity. On the other hand, isoeugenol degradation was clearly associated with increased reactivity for soft and hard nucleophiles. We previously isolated and identified isoeugenol's degradation products, including the main oxidized byproduct with superior thiol reactivity.[14] This reactive byproduct was structurally identified as *syn*-7,4′-oxyneolignan (**3a**) by comparison with the NMR data of 1,2-disubstituted-1-arylpropanes.[32] The comparison of probability analysis (CP3) and corrected mean absolute error (CMAE), based on the errors for each ^{1}H or ^{13}C chemical shifts between calculated and experimental values (Tables S2–S7), reaffirmed the unambiguous identification of *syn*-7,4′-oxyneolignan (**3a**) as the major isomer and the *anti*-diastereomer (**3b**) as a minor oxidative byproduct (Figures S5 and S6). Similarly to the NMR calculation of **3a**/**3b**, the *syn*-DCYA adduct **4** matches with 100% probability to the experimental data of **4a** [DP4+ (all (H and C) data) and Scaled DP4+ (all (H and C) data)] (Tables S8–S10 and Figures S7).

3.2. Non-animal Assessment of Skin Sensitization Potentials of Isoeugenol and Its Byproducts.

The electrophilic reactivity of a compound directly impacts the MIE,[5] but further cellular pathways must be activated for allergic contact dermatitis (ACD) to occur, irrespective of the fact that these pathways are triggered by the outcome of the MIE and do not involve the allergenic chemical. Characterization of the haptenation potential (key event 1) was performed using the DPRA method; whereas,activation of key events 2 and 3 was assessed *in vitro* using the KeratinoSens and the h-CLAT method, respectively, as adequate substitutive non-animal methods accepted by regulatory agencies. The results were subsequently integrated to gauge the ability of **3a** to promote the initiation of the

three key events. The skin sensitization results of isoeugenol samples before and after photo-induced oxidation are summarized in Table 1. Both oxidized isoeugenol and **3a** resulted in quantitative Cysdepletion in the DPRA, which agrees with the previously reported high-throughput screening HTS-DCYA data which ranked fresh isoeugenol, degraded isoeugenol, and 3a in order from weakest to strongest skin sensitizer.[14] Depletion of Lys-peptide was not quantifiable for 3a due to the instability of this compound under the reaction conditions and due to the formation of unresolved peaks near the Lys-peptide region in HPLC. In the KeratinoSens assay, the proinflammatory activities of isoeugenol after forced degradation and of compound 3a were comparable, with $EC_{1.5}$ of 10.9 and 13.2 μM, respectively. No activation of key event 3 was observed based on the expression of CD54 and CD86 markers in h-CLAT. When combining the experimental outcome with an integrated approach, 3a was classified as a strong potential skin sensitizer capable of activating key events 1 and 2 of the skin sensitization AOP (Table 1).

3.3. Thiol Reactivity of *syn*-7,4′-Oxyneolignan (3a).

The DPRA and HTS-DCYA methods provided orthogonal evidence of thiol depletion, but no structural information on the reactivity of **3a**, including reactive functional groups involved in the haptenation reaction, could be deduced. Considering this, the reactivity was further characterized using the NMR-DCYA method. The reaction between equimolar concentrations of **3a** with DCYA was completed within 40 min, resulting in quantitative formation of corresponding DCYA adducts (**4a** and **4b**; *syn*: *anti* = 9:1, Figures S2–S4) and an equimolar amount of isoeugenol (Figure 2). The relative configuration of the major adduct **4a** was confirmed to be *syn* by the CMAE and DP4+ probability analysis. In a similar fashion to the calculation of **3a**/**3b**, the *syn* configuration of the DCYA adduct **4** matches closely to the experimental data of **4a** with 100% probability [DP4+ (all (H and C) data) and scaled DP4+ (all (H and C) data)] (Tables S8–S10 and Figure S7).

A series of ^{1}H NMR experiments were conducted to establish the reaction kinetics and rate constants (Figure 3) to unravel the potential mechanism. As a result, the first-order plots of the log of [**3a**] and the log of [100-adducts] against time were more linear (R^2 = 0.999 and 0.997) than the second-order plots of 1/[**3a**] and 1/[100-adducts] (R^2 = 0.944 and 0.844). Thus, the nucleophilic substitution of **3a** with DCYA can be considered a first-order reaction with 0.054 s^{-1} as the rate constant. This was further confirmed by the identical k values for the **3a** depletion and DCYA adduct formation in the case of first-order plots.

Additionally, the stoichiometry of both reactants, **3a** and DCYA, was further investigated to establish their rate constants, in which the depletion rate of **3a** or the formation rate of the DCYA adduct was considered independent of DCYA concentration (Figure 4A,B). In contrast to the nucleophilic substitution of **3a**, the reaction rates were directly proportional to the concentration of **3a** (Figure 4C,D), reaffirming that the reaction proceeds as the first order in **3a** and zeroth-order in DCYA. Based on this evidence, reversible dissociation of **3a** to yield a short-lived reactive intermediate is proposed as the rate-determining step in the reaction (Figure 5), with the reaction between **3a** and DCYA proceeding through first-order kinetics *via* a reversible dissociation to a short-lived reactive species, which then reacts rapidly with DCYA to form **4a**/**4b**.

3.4. Diastereoselectivity and the Reactive Intermediate.

The selective generation of diastereomeric **4a** over **4b** can also serve as evidence for the first-order reaction kinetics of **3a** and the involvement of a short-lived reactive intermediate. A first-order reaction typically occurs with diastereomeric equilibrium; whereas, second-order reactions tend to be stereospecific with inversion of configuration.[33] The reaction of **3a** with DCYA proceeded with the selective formation of the *syn*-isomer with ≥90% diastereomeric excess (*d.e.*), independent of the reactant concentration or stoichiometry. Furthermore, the observed *d.e.* with *syn*-isomer preference is identical to the formation of 7,4′-oxyneolignans during the forced degradation of isoeugenol.[14] These observations suggest a clear *syn*-preference in the nucleophilic addition of DCYA or isoeugenol to form the corresponding adduct **4a** or **3a** *via* a common, short-lived intermediate. Based on the DFT calculations (Table S11), it is suggested that the *syn*-isomer (**3a**) is thermodynamically more stable than the corresponding *anti*-isomer (**3b**) by 1.19 kcal/mol (Figures S5 and S6), which rationalizes the experimentally observed diastereomeric excess. Moreover, to showcase the preferred antiperiplanar orientation of oxyneoliganans, select conformers of **3a** and **3b** were subjected to potential energy surface scans for the dihedral angle between -O-C7-C8-O- and calculated their relative total energies (Table S12 and Figures S9 and S10). All these select conformers prefer gauche orientation between the oxygen atom at C7 and the hydroxy group at C8.

To probe the possible role of the relative stereochemistry on reactivity, the minor isomer, *anti*-7,4′-oxyneolignan (**3b**) with DCYA, was also investigated. Interestingly, 3b also generated the same *syn*-DCYA adduct **4a** with d.e. >70%, and the observed diastereoselectivity was further confirmed by the DP4+ probability analysis. These data suggest that the nucleophilic addition of DCYA to either of the 7,4′-oxyneolignans, **3a** or **3b**, occurs *via* the same reactive intermediate, which we consider to be the hydroxyquinone methide (HQM). In hypothesis, the epoxide shown in Figure 5 could be the reactive intermediate, but we discount this possibility since **3a** or **3b** would each yield a single diastereospecific isomer with complete inversion at the C7 position. In contrast, the HQM can undergo Michael addition to yield a mixture of two adducts, the predominant product being the thermodynamically stable *syn*-adduct,[34,35] which is what was observed experimentally. However, formation of a HQM is plausible *via* direct deprotonation of a more acidic phenolic hydroxy group in **3a** (pK_a ca. 10), followed by a *retro*-1,6-Michael addition or *via* deprotonation of the less acidic aliphatic hydroxyl group (pK_a calculated by the method of Perrin et al.),[36] followed by intramolecular S_N2 displacement of the isoeugenol anion to form the transient epoxide which tautomerizes to the HQM. Both of these possibilities are shown in Figure 5. For the epoxide pathway to predominate, the intramolecular S_N2 reaction would have to be at least 10^4 times faster than the *retro*-1,6-Michael addition. While this is possible, we consider the *retro*-1,6-Michael addition to be the more likely scenario. Moreover, our findings indicate that it is the HQM, not the epoxide, that reacts with DCYA to form **4a** and **4b**.

4. DISCUSSION

The scope of the present work was to generate additional evidence to explain the elusive electrophilic chemistry of isoeugenol and its derivatives. The results presented herein diverge from the Bertrand *et al.*[6] hypothesis on the differential skin sensitization of eugenol and isoeugenol in terms of demethylation (eugenol) and formation of either the reactive *ortho*-quinone or the QM derived by the removal of two hydrogen atoms (isoeugenol). We provide direct experimental evidence of an alternative route involving a HQM to explain the stronger skin sensitization of isoeugenol. Skin sensitization assays show that degraded isoeugenol is a more potent skin sensitizer than fresh isoeugenol and that **3a** is more potent than degraded isoeugenol. Isolation, characterization, and thiol reactivity of **3a** exemplify the role of a transient reactive HQM intermediate specific to isoeugenol. The forced degradation studies of isoeugenol indicate that the position of the double bond has significant consequences on the stability of **1**, leading to the formation of **3a**.

The key difference between eugenol and isoeugenol is that the exocyclic double bond is conjugated with the aromatic ring in isoeugenol, which facilitates epoxidation. This forms a transient epoxide that can tautomerize *via* proton transfer to an electrophilic quinone methide, the HQM.

The most direct explanation of increased skin sensitization is that a short-lived isoeugenol epoxide might be formed, followed by isomerization to an HQM intermediate. This HQM intermediate can react rapidly with isoeugenol to form **3a** (plus **3b**). Kinetic and computational studies on the reactivity of **3a** support the hypothesis of the HQM as a putative reactive intermediate in nucleophilic additions. Compounds **3a** and **3b** themselves can be envisioned as byproducts of the same type of chemistry, where the HQM resulting from epoxidation of the isoeugenol double bond can react with a second molecule of isoeugenol to generate **3a** and **3b**, but predominantly the *syn*-isomer **3a**. A similar rationale would not apply to eugenol as it lacks conjugation and would not produce similar reactive intermediates. A plausible eugenol epoxide derivative would not be able to promptly rearrange and react with thiols. Indeed, eugenol epoxide was synthesized, characterized successfully, and utilized in several organic reactions.[37–39] These findings align with previously reported evidence that conjugated dienes, in which at least one of the double bonds is cyclic, could sensitize skin *via* oxidation to an epoxide.[40]

The same analogy can be applied to isoeugenol's oxidation under (a)biotic conditions. Isoeugenol can be transformed in the epidermis (abiotically or enzymatically), leading to the transient HQM species *via* epoxide formation, which can further react with skin proteins. Moreover, asecond molecule of isoeugenol can react with the HQM to generate **3a**/**3b**, and the experimental evidence suggests that these neolignans would decompose to the same reactive intermediate HQM. The observed sensitization by isoeugenol can be considered a combination of these two mechanistic pathways, both of which involve the same ultimate hapten, the HQM (Figure 6). Neither of the two pathways have been unequivocally established as the dominant. Furthermore, we cannot exclude the possibility that the dimer is formed due to abiotic oxidation of isoeugenol on the skin surface, especially considering

that the relatively high surface-to-volume ratio may promote faster oxidation than when isoeugenol is exposed to photo-induced oxidation in the laboratory.

Herein we have considered three distinct potential mechanisms for the skin sensitizing properties of isoeugenol. The first involves oxidative demethylation of the -OMe group and further oxidation to an *ortho*-quinone. This mechanism does not appear compatible with the evidence of Bertrand et al. for isoeugenol, though it is compatible with their evidence for eugenol. The second proposed mechanism involves oxidation by removal of a hydrogen atom from the $–C_3H_5$ group to result in a *para*-quinone methide. This mechanism has been proposed for isoeugenol, but a third mechanism with eugenol could also react similarly to form the same *para*-quinone methide. This study proposes that isoeugenol, either directly or through an oxidative dimer, may form a transient epoxide intermediate that quickly isomerizes to a reactive HQM. None of these hypotheses can be completely ruled out, but the current findings enable the best and most straightforward explanation of why isoeugenol and eugenol, similar in their structures, are different in their skin sensitization properties..

Supplementary Material

Refer to Web version on PubMed Central for supplementary material.

ACKNOWLEDGMENTS

This article is dedicated to the memory of our beloved mentor Professor Jon F. Parcher. This research was supported in part by “Science-Based Authentication of Botanical Ingredients”, funded by the Center for Food Safety and Applied Nutrition, US Food and Drug Administration grant number 5U01FD004246. We would like to thank the Mississippi Center for Supercomputing Research and NSF MRI 1338056 for providing access to supercomputer resources.

ABBREVIATIONS

ACD	allergic contact dermatitis
ACN	acetonitrile
CMAE	corrected mean absolute error
AOP	adverse outcome pathway
Cys	cysteine
DBN	1,5-diazabicyclo[4.3.0]non-5-ene
DCYA	dansyl cysteamine
DFT	density functional theory
DMSO	dimethyl sulfoxide
DPRA	direct peptide reactivity assay
h-CLAT	human cell line activation assay
HTS-DCYA	high-throughput screening using dansyl cysteamine

HQM	hydroxy quinone methide
IFRA	International Fragrance Association
IS	internal standard
KE	key event
Lys	lysine
MeOH	methanol
MIE	molecular initiating event
NMR	nuclear magnetic resonance
NMR-DCYA	NMR-based in chemico method using dansyl cysteamine
OECD	Organisation for Economic Co-operation and Development
QM	quinone methide
RFIs	relative fluorescence intensities

REFERENCES

(1). Chatterjee D; Bhattacharjee P Use of eugenol-lean clove extract as a flavoring agent and natural antioxidant in mayonnaise: product characterization and storage study. J. Food Sci. Technol. 2015, 52, 4945–4954. [PubMed: 26243914]

(2). Koeduka T; Fridman E; Gang DR; Vassao DG; Jackson BL; Kish CM; Orlova I; Spassova SM; Lewis NG; Noel JP; Baiga TJ; Dudareva N; Pichersky E Eugenol and isoeugenol, characteristic aromatic constituents of spices, are biosynthesized via reduction of a coniferyl alcohol ester. Proc. Natl. Acad. Sci. U.S.A. 2006, 103, 10128–10133. [PubMed: 16782809]

(3). Rastogi SC; Johansen JD Significant exposures to isoeugenol derivatives in perfumes. Contact Dermatitis 2008, 58, 278–281. [PubMed: 18416757]

(4). White JM; White IR; Glendinning A; Fleming J; Jefferies D; Basketter DA; McFadden JP; Buckley DA Frequency of allergic contact dermatitis to isoeugenol is increasing: a review of 3636 patients tested from 2001 to 2005. Br. J. Dermatol. 2007, 157, 580–582. [PubMed: 17573874]

(5). Organisation for Economic Co-operation and Development. The Adverse Outcome Pathway for Skin Sensitisation Initiated by Covalent Binding to Proteins; OECD Publishing, 2014.

(6). Bertrand F; Basketter DA; Roberts DW; Lepoittevin JP Skin sensitization to eugenol and isoeugenol in mice: possible metabolic pathways involving ortho-quinone and quinone methide intermediates. Chem. Res. Toxicol. 1997, 10, 335–343. [PubMed: 9084914]

(7). Urbisch D; Becker M; Honarvar N; Kolle SN; Mehling A; Teubner W; Wareing B; Landsiedel R Assessment of pre- and prohaptens using nonanimal test methods for skin sensitization. Chem. Res. Toxicol. 2016, 29, 901–913. [PubMed: 27070937]

(8). Marzulli FN; Maibach HI Contact allergy: predictive testing of fragrance ingredients in humans by Draize and Maximization methods. J. Environ. Pathol. Toxicol. 1980, 3, 235–245. [PubMed: 7441083]

(9). Johansen JD; Menne T The fragrance mix and its constituents: a 14-year material. Contact Dermatitis 1995, 32, 18–23. [PubMed: 7720365]

(10). Barratt MD; Basketter DA Possible origin of the skin sensitization potential of isoeugenol and related compounds. (I). Preliminary studies of potential reaction mechanisms. Contact Dermatitis 1992, 27, 98–104. [PubMed: 1395636]

(11). Basketter D; Gerberick G; Kimber I; Loveless S The local lymph node assay: a viable alternative to currently accepted skin sensitization tests. Food Chem. Toxicol. 1996, 34, 985–997. [PubMed: 9012774]

(12). Scholes EW; Pendlington RU; Sharma RK; Basketter DA Skin metabolism of contact allergens. Toxicol. In Vitro 1994, 8, 551–553. [PubMed: 20692958]

(13). Patlewicz G; Casati S; Basketter DA; Asturiol D; Roberts DW; Lepoittevin JP; Worth AP; Aschberger K Can currently available non-animal methods detect pre and pro-haptens relevant for skin sensitization? Regul. Toxicol. Pharmacol. 2016, 82, 147–155. [PubMed: 27569201]

(14). Ahn J; Avonto C; Chittiboyina AG; Khan IA Is Isoeugenol a prehapten? Characterization of a thiol-reactive oxidative byproduct of isoeugenol and potential implications for skin sensitization. Chem. Res. Toxicol. 2020, 33, 948–954. [PubMed: 32119530]

(15). Oka Y; Nakamura A; Watanabe H; Touhara K An odorant derivative as an antagonist for an olfactory receptor. Chem. Senses 2004, 29, 815–822. [PubMed: 15574817]

(16). Avonto C; Wang M; Chittiboyina AG; Vukmanovic S; Khan IA Chemical stability and in chemico reactivity of 24 fragrance ingredients of concern for skin sensitization risk assessment. Toxicol. In Vitro 2018, 46, 237–245. [PubMed: 28927722]

(17). Chittiboyina AG; Avonto C; Khan IA What happens after activation of ascaridole? Reactive compounds and theiriImplications for skin sensitization. Chem. Res. Toxicol. 2016, 29, 1488–1492. [PubMed: 27513446]

(18). Chittiboyina AG; Avonto C; Rua D; Khan IA Alternative testing methods for skin sensitization: NMR spectroscopy for probing the reactivity and classification of potential skin sensitizers. Chem. Res. Toxicol. 2015, 28, 1704–1714. [PubMed: 26225548]

(19). Avonto C; Chittiboyina AG; Wang M; Vasquez Y; Rua D; Khan IA In Chemico evaluation of tea tree essential oils as skin sensitizers: Impact of the chemical composition on aging and generation of reactive species. Chem. Res. Toxicol. 2016, 29, 1108–1117. [PubMed: 27286037]

(20). Avonto C; Rua D; Lasonkar PB; Chittiboyina AG; Khan IA Identification of a compound isolated from German chamomile (Matricaria chamomilla) with dermal sensitization potential. Toxicol. Appl. Pharmacol. 2017, 318, 16–22. [PubMed: 28109818]

(21). Smith SG; Goodman JM Assigning the stereochemistry of pairs of diastereoisomers using GIAO NMR shift calculation. J. Org. Chem. 2009, 74, 4597–4607. [PubMed: 19459674]

(22). Grimblat N; Zanardi MM; Sarotti AM Beyond DP4: An improved probability for the stereochemical assignment of isomeric compounds using quantum chemical calculations of NMR shifts. J. Org. Chem. 2015, 80, 12526–12534. [PubMed: 26580165]

(23). Duddupudi AL; Pandey P; Vo H; Welsh CL; Doerksen RJ; Cuny GD Hypervalent iodine mediated oxidative cyclization of acrylamide N-carbamates to 5,5-disubstituted oxazolidine-2,4-diones. J. Org. Chem. 2020, 85, 7549–7557. [PubMed: 32392063]

(24). Zou Y; Wang X; Sims J; Wang B; Pandey P; Welsh CL; Stone RP; Avery MA; Doerksen RJ; Ferreira D; Anklin C; Valeriote FA; Kelly M; Hamann MT Computationally assisted discovery and assignment of a highly strained and PANC-1 selective alkaloid from Alaska's deep ocean. J. Am. Chem. Soc. 2019, 141, 4338–4344. [PubMed: 30758203]

(25). Roos K; Wu C; Damm W; Reboul M; Stevenson JM; Lu C; Dahlgren MK; Mondal S; Chen W; Wang L; Abel R; Friesner RA; Harder ED OPLS3e: Extending force field coverage for drug-like small molecules. J. Chem. Theory Comput. 2019, 15, 1863–1874. [PubMed: 30768902]

(26). Wolinski K; Hinton JF; Pulay P Efficient implementation of the gauge-independent atomic orbital method for NMR chemical shift calculations. J. Am. Chem. Soc. 1990, 112, 8251–8260.

(27). Tomasi J; Mennucci B; Cammi R Quantum mechanical continuum solvation models. Chem. Rev. 2005, 105, 2999–3094. [PubMed: 16092826]

(28). Bergström MA; Ott H; Carlsson A; Neis M; Zwadlo-Klarwasser G; Jonsson CA; Merk HF; Karlberg A-T; Baron JM A skin-like cytochrome P450 cocktail activates prohaptens to contact allergenic metabolites. J. Invest. Dermatol. 2007, 127, 1145–1153. [PubMed: 17124504]

(29). Natsch A; Haupt T; Laue H Relating Skin Sensitizing Potency to Chemical Reactivity: Reactive Michael Acceptors Inhibit NF-κB Signaling and Are Less Sensitizing than S_NAr- and S_N2-Reactive Chemicals. Chem. Res. Toxicol. 2011, 24, 2018–2027. [PubMed: 22023385]

(30). Duisken M; Sandner F; Blömeke B; Hollender J Metabolism of 1, 8-cineole by human cytochrome P450 enzymes: identification of a new hydroxylated metabolite. Biochim. Biophys. Acta, Gen. Subj. 2005, 1722, 304–311.

(31). Smith CK; Moore CA; Elahi EN; Smart AT; Hotchkiss SA Human skin absorption and metabolism of the contact allergens, cinnamic aldehyde, and cinnamic alcohol. Toxicol. Appl. Pharmacol. 2000, 168, 189–199. [PubMed: 11042091]

(32). Schmid GH Determination of erythro and threo configurations by nuclear magnetic resonance spectroscopy. Can. J. Chem. 1968, 46, 3415–3418.

(33). Soderberg T Organic Chemistry with a Biological Emphasis, 2019; Vol. I.

(34). Parra A; Tortosa M para-Quinone methide: A new player in asymmetric catalysis. ChemCatChem 2015, 7, 1524–1526.

(35). Zhu X; Akiyama T; Yokoyama T; Matsumoto Y Lignin-biosynthetic study: Reactivity of quinone methides in the diastereopreferential formation of p-hydroxyphenyl- and guaiacyl-type β-O-4 structures. J. Agric. Food Chem. 2019, 67, 2139–2147. [PubMed: 30668903]

(36). Perrin DD; Dempsey B; Serjeant EP pKa Prediction for Organic Acids and Bases; Chapman and Hall: London, 1980. eBook ISBN: 978-94-009-5883-8.

(37). Elgendy EM; Khayyat SA Oxidation reactions of some natural volatile aromatic compounds: anethole and eugenol. Russ. J. Org. Chem. 2008, 44, 823–829.

(38). Genc Bilgicli H; Ergon D; Taslimi P; Tuzun B; Akyazi Kuru I; Zengin M; Gulcin I Novel propanolamine derivatives attached to 2-metoxifenol moiety: Synthesis, characterization, biological properties and molecular docking studies. Bioorg. Chem. 2020, 101, 103969. [PubMed: 32474181]

(39). Yadav RN; K Banik B Studies on natural products: a facile epoxidation of eugenol. Mod. Chem. Appl. 2018, 06, 1000255.

(40). Bergström MA; Luthman K; Nilsson JLG; Karlberg A-T Conjugated dienes as prohaptens in contact allergy: in vivo and in vitro studies of structure-activity relationships, sensitizing capacity, and metabolic activation. Chem. Res. Toxicol. 2006, 19, 760–769. [PubMed: 16780354]

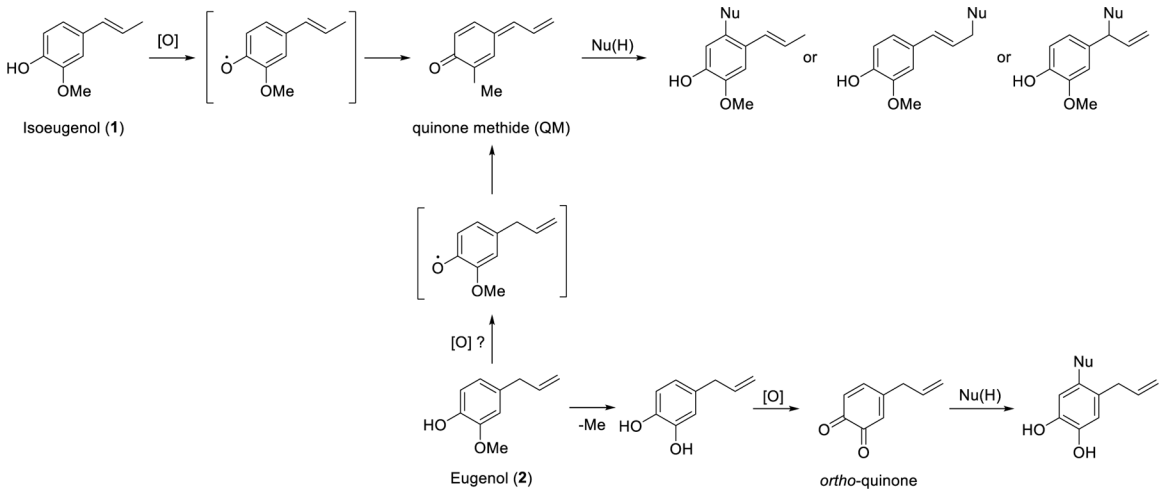

Figure 1.

ortho-Quinone and quinone methide (QM) pathway: the skin sensitization potential of isoeugenol and eugenol and involvement of potential reactive intermediates as proposed by Bertrand *et al.*[6]

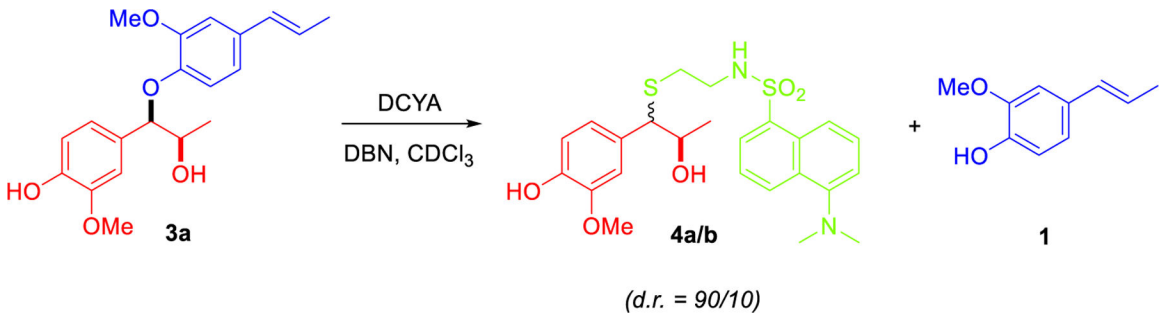

Figure 2.

Nucleophilic reaction between DCYA and *syn*-7,4′-oxyneolignan (**3a**) and regeneration of isoeugenol.

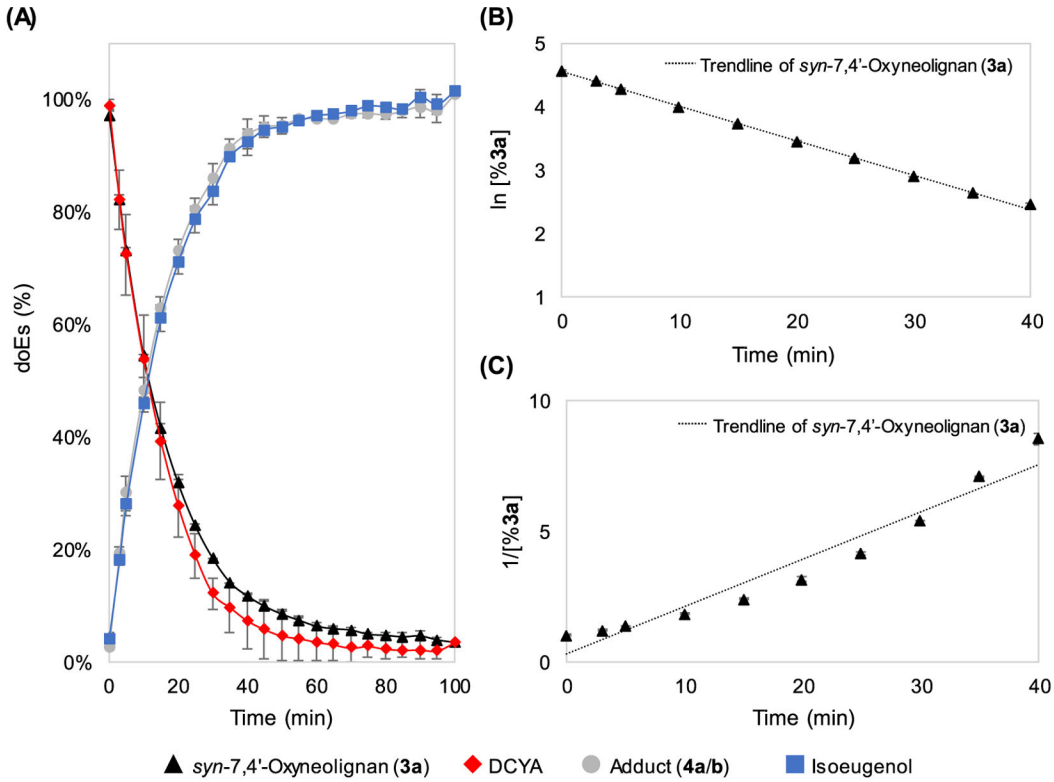

(D)

	First order plot				Second order plot			
	3a	**DCYA**	**100-Adduct**	**100-IE**	**3a**	**DCYA**	**100-Adduct**	**100-IE**
Rate constants, k (s^{-1})	0.054	0.067	0.068	0.063	0.183	0.298	0.332	0.272
R^2	0.999	0.997	0.997	0.997	0.944	0.904	0.844	0.864

Figure 3.

^{1}H NMR kinetic experiments between *syn*-7,4′-oxyneolignan (**3a**) and DCYA (1:1) using the NMR-DCYA method. (A) Relative ratios of depletion of DCYA (red) and **3a** (black) as well as the formation of the adduct (gray) and isoeugenol (blue); (B) kinetic plot of 3a according to the first-order reaction; (C) kinetic plot of **3a** according to the second-order reaction; and (D) rate constants (k) and coefficient correlation of determination (R^2) for each plot.

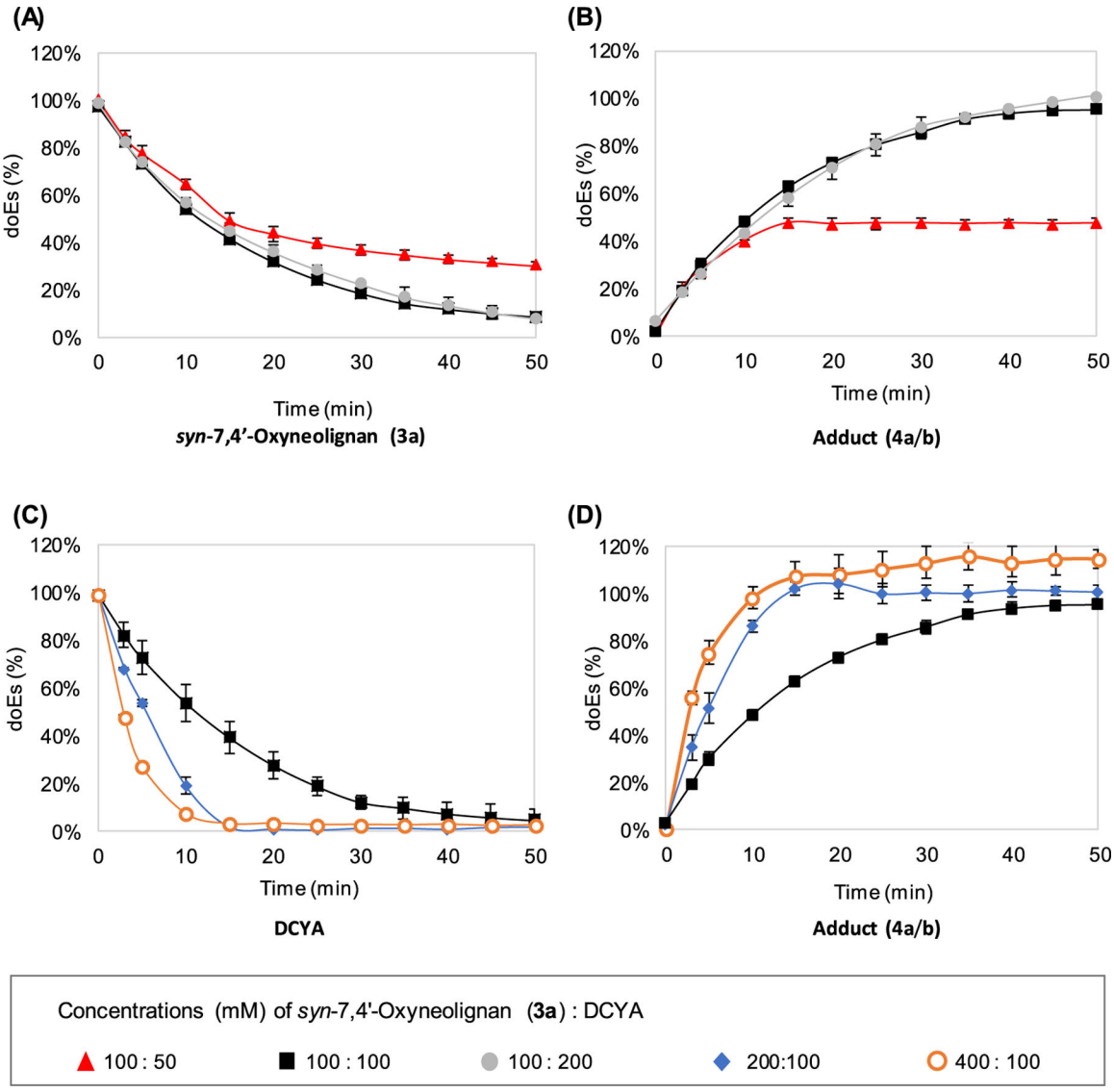

Figure 4.

Kinetic NMR results of DCYA addition to **3a**. Depletion of **3a** (A) and formation of DCYA-adducts (B) at increasing concentrations of DCYA; depletion of DCYA (C) and formation of DCYA-adducts (D) at increasing concentrations of **3a**. Kinetic NMR results for **3b** provided in the Supporting Information as Figure S8.

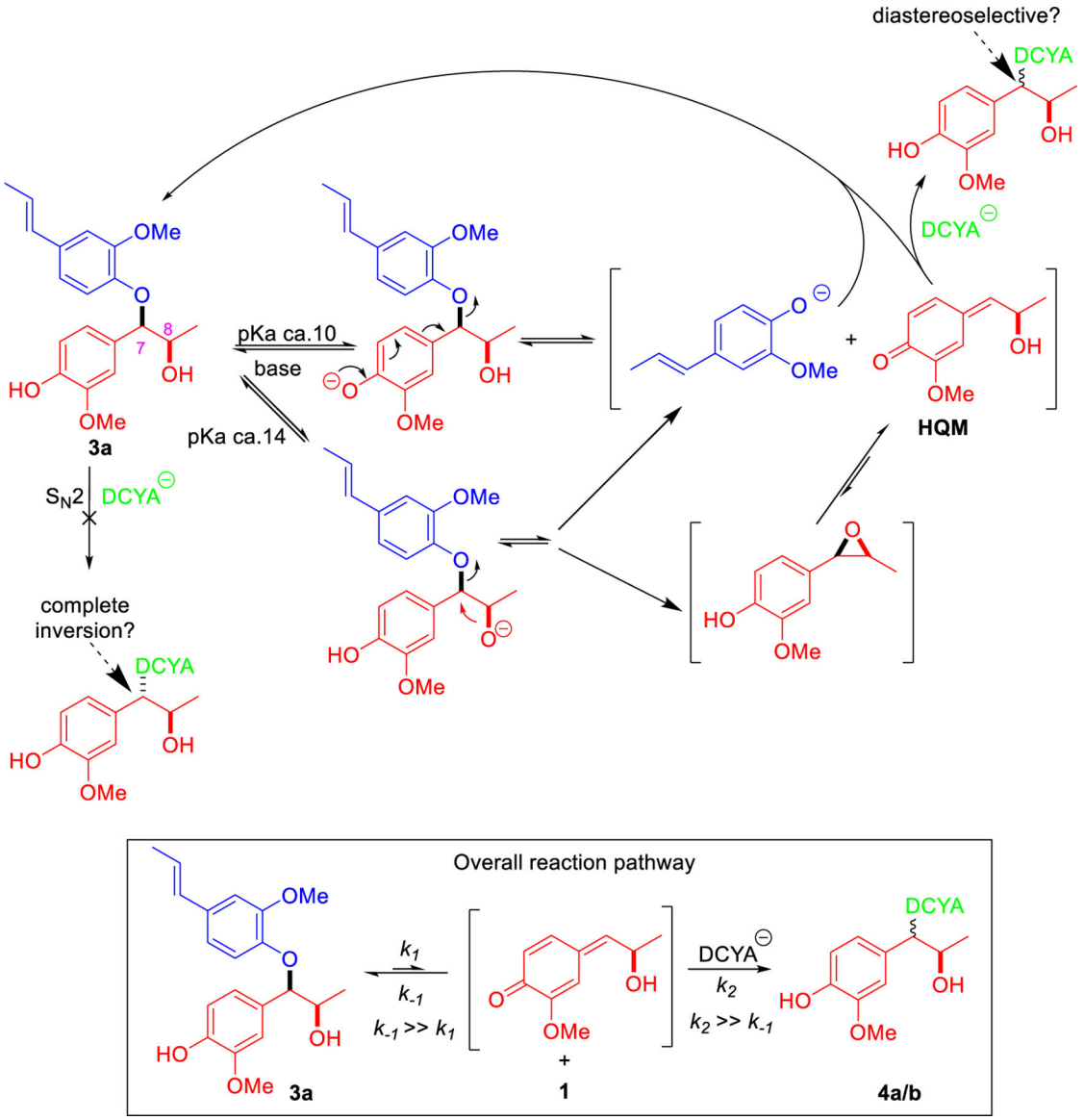

Figure 5.

Potential reaction pathway for the thiol reactivity of *syn*-7,4′-oxyneolignan (**3a**) with DCYA.

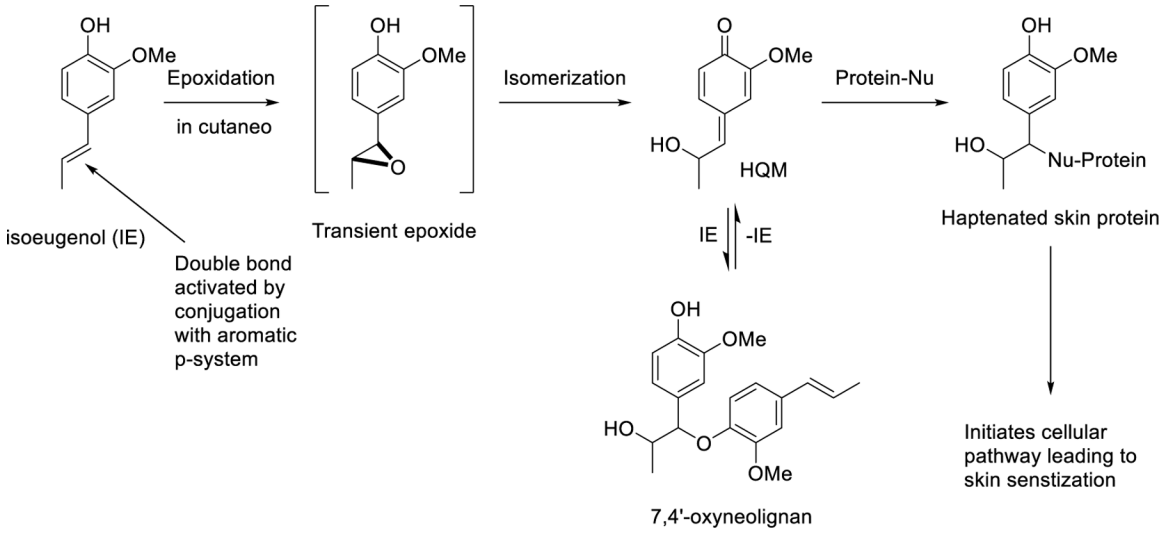

Figure 6.
Proposed chemical pathway for isoeugenol's skin sensitization.

Table 1.

Non-animal Skin Sensitization Results for Isoeugenol and 3a

Compound		DCYA (RI)[a]	DPRA (% dep)		KeratinoSens		h-CLAT		
			Cys	Lys	$EC_{1.5}$ (μM)	TC_{50} (μM)	CD54	CD86	CV75 (μg/mL)
Isoeugenol	before degradation	21.6 ± 2[a]	28.3 ± 4	2.3 ± 1	3.9 ± 0	255 ± 5	negative	negative	125
	after degradation	62.9 ± 4[a]	97.4 ± 0	−2.2 ± 2	10.9 ± 2	275 ± 25	negative	negative	125
syn-7,4′-Oxyneolignan(**3a**)		116.6 ± 5[a]	91.5 ± 2	n.q	13.2 ± 1		negative	negative	250

[a]Ahn et al. (2020).

n.q. = not quantifiable.